I R A M P
16(1), Jan 2025, pp. 15-28

ISSN: 2229-39-44

The Dirac Equation Inside the Proton of Hydrogen Atoms: the Non-Analytic Solution and its Application to the Experimental Verification of the Two-Body Decay of Neutrons

EUGENE OKS

Physics Department, 380 Duncan Drive, Auburn University, Auburn, AL 36849, USA
Corresponding author email: oksevgu@auburn.edu

ABSTRACT: In one of our previous papers, we obtained a general class of potentials inside the nucleus, such that the singular solution of the Dirac equation for the S-states of hydrogen atoms outside the nucleus can be matched with the corresponding regular solution inside the nucleus (the proton) at the boundary. The experimental charge density distribution inside the proton generates a particular case of such potentials inside the proton. In this way, it was predicted the existence of the second kind of hydrogen atoms: the atoms having only the S-states, the states being characterized by the singular solution of the Dirac equation outside the proton (these kind of atoms were later called the second flavor of hydrogen atoms abbreviated as SFHA). This theoretical prediction was then evidenced by several different types of atomic experiments and by astrophysical observations. We show that such solution inside the proton can be (and is) found within the class of functions that are *non-analytic* at r = 0 – in distinction to the traditional practice of limiting the search for the solution by the class of analytic functions, i.e., by functions that can be adequately represented by their expansion into the Laurent series. We apply the obtained results for resolving the neutron lifetime puzzle: the puzzle consisting in the discrepancy between the neutron lifetime measured in two different types of experiments, the discrepancy being well beyond the experimental error margins. We show that the two-body decay of neutrons produces overwhelmingly the SFHA (rather than the usual hydrogen atoms). By demonstrating that the enhanced in this way branching ratio for the 2-body decay of neutrons (compared to the 3-body decay) is in the excellent agreement with the branching ratio required for reconciling the neutron lifetime values measured in the trap and beam experiments, we completely resolve the above discrepancy. Finally, we provide the conceptual designs of the experiment that would constitute both the first detection of the two-body decay of neutrons and the verification that that the two-body decay of neutrons produces overwhelmingly the SFHA. Thus, our results seem to be important both from the theoretical and experimental viewpoints.

Keywords: Dirac equation; non-analytic solution; second flavor of hydrogen atoms; two-body decay of neutrons; designs of the experimental confirmation of neutrons two-body decay; dark matter

1. INTRODUCTION

Analysis of atomic experiments related to the distribution of the linear momentum in the ground state of hydrogen atoms revealed an enormous discrepancy: the ratio of the experimental and previous theoretical results was up to *tens of thousands* [1]. Namely, the experimental High-energy Tail of the Momentum Distribution (HTMD) [2] for large momenta p falls off much-much slower than the theoretical one [3].

This was the motivation behind our *theoretical* results from paper [1]. There are two analytical solutions of the standard Dirac equation of quantum mechanics for hydrogen atoms: 1) the solution that is weakly singular at small r; 2) the solution that is more strongly singular at small r. The radial part of the coordinate wave functions for the ground state has the following scaling at small r:

$$R_{0,-1}(r) \propto 1/r^{q}, \quad q = 1 \pm (1 - \alpha^2)^{1/2}. \tag{1}$$

Here α is the fine structure constant; -1 in the subscript of the wave function $R_{0,-1}$ is the eigenvalue of the operator $K = \beta(2\mathbf{Ls} + 1)$ that commutes with the Hamiltonian; β is the Dirac matrix of the rank 4; **s** and **L** are the spin and orbital angular momenta operators, respectively.

Thus, the first solution is characterized by only a weak singularity: $q \approx \alpha^2/2 \approx 0.000027$ (hereafter, the "regular" solution, for brevity). The second solution is significantly singular ($q \approx 2$) and it is usually rejected, the reason being the divergence of the normalization integral at $r = 0$.

However, the allowance for the finite nuclear size changes the situation. In paper [1] we obtained a general class of potentials inside the nucleus, such that the singular solution outside the nucleus can be in fact matched with the corresponding regular solution inside the nucleus at the boundary. Specifically, in that paper there was considered an arbitrary spherically-symmetric interaction potential V(r), having two different shapes in the interior region $r < R$ and in the exterior region $r > R$. It was demonstrated that the singular solution in the exterior region can be matched at the boundary with the regular solution at the interior region for the class of potentials satisfying the following condition (written in the natural units $\hbar = m_e = c = 1$)

$$\int_0^R V(r')\, r'^2\, dr' + (1 - E)r^3/3 \approx \{\int_R^\infty [V(r')/ r'^2]dr' - (1 + E)/r\}^{-1}. \tag{2}$$

In Eq. (2), E is the total energy of the atomic electron, including the rest energy.

Potentials in the interior region satisfying Eq. (2) should rapidly rise toward the boundary $r = R$. Charge Density Distributions (CDDs) that have the maximum at $r = 0$ and falls off to the periphery yield one particular case of such potentials.

The CDD inside protons does have the maximum at $r = 0$ and falls off to the periphery. This is well-known since 1980s from the experiment on the elastic scattering of electrons on protons – see, e.g., works [4-6]. Thus, the singular solution of the Dirac equation outside the proton can be matched with the regular solution of the Dirac equation inside the proton at the boundary.

So, in paper [1] we derived analytically the corresponding wave function. As a result, the huge multi-order discrepancy between the experimental and theoretical HTMD got completely eliminated. Here is why: for the singular solution outside the proton, a much stronger rise of the coordinate wave function toward the proton at small r translates into a *much slower fall-off* of the wave function in the p-representation for large p – according to the properties of the Fourier transform.

The derivation of the corresponding wave function in paper [1] utilized only the fact that the eigenvalue of the operator K in the ground state is $k = -1$. Therefore, in fact, the corresponding derivation is valid for all states of hydrogen atoms having the quantum number $k = -1$.

Such states are the S-states: the states where the orbital angular momentum l is equal to zero. Thus, both the singular and regular solution of the Dirac equation outside the proton are permissible for all S-states, as well as for the states of the continuous spectrum having $l = 0$ [7].

This second type of hydrogen atoms that have only the S-states was later named the Second Flavor of Hydrogen Atoms, hereafter SFHA [8]. The reason is explained below.

Both the regular and singular solutions of the Dirac equation outside the proton correspond to the *same energy*. Since this means the *additional degeneracy*, then according to the fundamental theorem of quantum mechanics, there should be an *additional conserved quantity*. In other words: hydrogen atoms have two flavors**,** differing by the eigenvalue of this additional, new conserved quantity: hydrogen atoms have *flavor symmetry* [8]. It is called so by analogy with quarks that have flavors: for example, there are up and down quarks.

Thus, the elimination of the huge multi-order discrepancy between the theoretical and experimental distributions of the linear momentum in the ground state of hydrogen atoms constituted *the first experimental evidence of the existence of the SFHA* – since no alternative explanation for this huge discrepancy was ever provided. By now there are two *additional experimental evidences* from two different kinds of atomic experiments: from electron impact excitation of hydrogen atoms and from electron impact excitation of hydrogen molecules. For *both kinds of the experiments, the SFHA-based explanation removed large discrepancies (up to a factor of two or more*) between the experimental and previous theoretical results, while alternative explanations were never provided.

The *primary feature* of the SFHA is the following. Since the SFHA have only the S-states, then according to the well-known selection rules of quantum mechanics, *the SFHA do not emit or absorb the electromagnetic radiation* – they remain *dark*. More details: due to the selection rules, all matrix elements (both diagonal and non-diagonal) of the operator **d** of the electric dipole moment are zeros. For this reason, the SFHA do not couple not only to the dipole radiation, but also to the quadrupole, octupole, and all higher multipole terms – because multipoles contain linear combinations of various powers of the radius-vector operator **r** of the atomic electron, which yield zeros in all orders of the perturbation theory for the SFHA. For the same reason, the SFHA cannot exhibit multi-photon transitions.This is because multi-photon transitions consist of several one-photon virtual transitions, each step being controlled by a matrix element of **r**, but all these matrix elements are zeros for the SFHA.

For the above reasons, the SFHA does not react to a static electric field or a laser field – no static or dynamic Stark effect. Therefore, the SFHA *cannot be excited or ionized by a static electric field or by a laser field*, though it can be excited or ionized, e.g., by an electron beam.

There is also an astrophysical evidence that SFHA exists. There is a perplexing observation by Bowman et al [9] of the anomalous absorption in the (redshifted) 21 cm line from the early Universe. The absorption signal was found to be *2 to 3 times stronger* than predicted by the standard cosmology. This indicated that the hydrogen gas temperature was significantly smaller than predicted by the standard cosmology.

Barkana [10] suggested that some *unspecified Dark Matter (DM)* particles provided an additional cooling of the hydrogen gas by collisions. By his estimates, the quantitative explanation of the above anomalous absorption required the mass of unspecified DM particles to be of the order of the baryons masses, so that the explanation required unspecified *baryonic* DM *particles*. Thereafter McGaugh [11] examined the results by Bowman et al [9] and by Barkana [10], and came to the same conclusion: the explanation of the anomalous absorption requires baryonic DM particles.

In paper [7] we considered the following: what if these unspecified DM particles were the SFHA? In that paper it was explained that during the expansion of the Universe, the SFHA decouple from the cosmic microwave background radiation (due to having only the S-states) *earlier* than the usual hydrogen atoms. For this reason, their spin temperature (controlling the absorption signal in the 21 cm line) was smaller than for the usual hydrogen atoms. This explained the observed anomalous absorption both qualitatively and quantitatively and made the *SFHA a compelling candidate for the baryonic DM*.

Indeed, from astrophysical observations it is known that the ratio R_1 = (nonbarDM)/(barDM) ~ 5 and that the ratio R_2 = (totalDM)/UM= (nonbarDM + barDM)/UM. Here nonbarDM, barDM, totalDM, and UM stand for nonbaryonic DM, baryonic DM, total DM, and the Usual Matter, respectively. Since $R_1 \sim R_2$, then it is easy to find out the following:

UM ~ barDM(nonbarDM + barDM)/nonbarDM = barDM(1 + barDM/nonbarDM) ~ (6/5)barDM. Therefore, the ratio R_3 = (barDM)/UM ~ 5/6 ~ 0.8.

The experimental ratio of the SFHA to the usual hydrogen atoms from atomic experiments evidenced the existence of the SFHA is R_4 = SFHA/(usual H) ~ (0.5 – 1). The hydrogen abundance in the universe is known to be 74%. Therefore, R_5 = SFHA/[(usual H) + (other chemical elements)] ~ (0.4 – 0.7). But R_5 *is the same as SFHA/UM* and is ~ (0.4 – 0.7). So, from the comparison of the atomic physics experimental ratio R_5 = SFHA/UM ~ (0.4

– 0.7) with the corresponding astrophysical ratio R_3 = (barDM)/UM ~ 0.8 follows: *the SFHA seems to comprise most of the baryonic DM in the current epoch* [11].

It is important to underscore that the theory of the SFHA is based on the *standard quantum mechanics* (the Dirac equation). It does not require going beyond the Standard Model of particle physics and it does not recourse to changing the physical laws – in distinction to the overwhelming majority of dark matter models.

In the present paper we derive the explicit form of the solution of the Dirac equation inside the proton for the S-states – the solution that at the proton boundary matches the corresponding singular solution, as required by quantum mechanics: both the wave function and its derivative are continuous at the boundary. We show that such solution inside the proton can be (and is) found within the class of functions that are *non-analytic* at r = 0 – in distinction to the traditional practice of limiting the search for the solution by the class of analytic functions, i.e., by functions that can be adequately represented by their expansion into the Laurent series.

Next, we apply the obtained results for resolving the neutron lifetime puzzle: the puzzle consisting in the discrepancy between the neutron lifetime measured in two different types of experiments, the discrepancy being well beyond the experimental error margins. We show that the 2-body decay of neutrons produces overwhelmingly the SFHA (rather than the usual hydrogen atoms). By demonstrating that the enhanced in this way branching ratio for the 2-body decay of neutrons (compared to the 3-body decay) is in the excellent agreement with the branching ratio required for reconciling the neutron lifetime values measured in the trap and beam experiments, we completely resolve the above discrepancy.

Finally, we provide the conceptual designs of the experiment that would constitute both the first detection of the two-body decay of neutrons and the verification that that the two-body decay of neutrons produces overwhelmingly the SFHA.

In Appendix A, we offer details on the experimental charge distribution inside the proton.

2. ANALYTIC SOLUTION OF THE DIRAC EQUATION INSIDE THE PROTON FOR THE S-STATES OF HYDROGEN ATOMS

For hydrogen atoms, the Dirac equation for the f- and g-components of the Dirac bispinor has the form (in the natural units) – see, e.g., the textbook [13] :

$$df(r)/dr = (k - 1)f(r)/r - h_1(r)g(r), \tag{3}$$

$$dg(r)/dr = h_2(r)f(r) - (k + 1)g(r)/r, \tag{4}$$

where

$$h_1(r) = W - 1 - V(r),\ h_2(r) = W + 1 - V(r). \tag{5}$$

In Eq. (5), W is the energy and V(r) is the potential energy of the atomic electron. In Eqs. (3) and (4), k is the eigenvalue of the following operator

$$K = b(2\mathbf{Ls} + 1) \tag{6}$$

that commutes with the Hamiltonian. In Eq. (6), b is the Dirac matrix of the rank 4, **L** and **s** are the operators of the orbital and spin momenta, respectively.

For the S-states (on which we focus in the present paper), k = – 1. Then from Eq. (4) we find:

$$f(r) = [dg(r)/dr]/h_2(r). \tag{7}$$

On substituting Eq. (7) in Eq. (3), we obtain:

$$r(d^2g/dr^2) + [2 + r(dV/dr)/h_2(r)](dg/dr) + rh_1(r)h_2(r)g = 0. \tag{8}$$

Now we study this equation and its solution near the origin, i.e., near r = 0. After denoting

$$V_0 = -|V(0)| = \text{const} > 0, \tag{9}$$

Eqs. (7) and (8) can be simplified as follows:

$$r[d^2g(r)/dr^2) + 2[dg(r)/dr] + hrg(r) = 0, \tag{10}$$

$$f(r) = [dg(r)/dr]/h_{20}, \tag{11}$$

where

$$h = (W + V_0)^2 - 1 = \text{const}, \; h_{20} = W + 1 + V_0 = \text{const}. \tag{12}$$

We start from the traditional practice of limiting the search for the solutions by the class of analytic functions, i.e., by functions that can be adequately represented by their expansion into the Laurent series. Namely, we seek the solutions in the form:

$$g(r) = r^d \sum_{m=0}^{\infty} a_m r^m, \tag{13}$$

where a_m = const for any n and d = const. On substituting Eq. (13) in Eq. (10) and requesting the mutual cancellation of the lowest powers of r, we find:

$$d(d + 1) = 0, \tag{14}$$

so that $d_1 = 0$ and $d_2 = -1$.

For the solution with $d_1 = 0$, corresponding to

$$g_1(r) \approx a_0, \tag{15}$$

from Eq. (11) we get:

$$f_1(r) \approx a_1/h_{20}. \tag{16}$$

For the solution with $d_2 = -1$, corresponding to

$$g_2(r) \approx a_0/r, \tag{17}$$

from Eq. (11) we obtain:

$$f_2(r) \approx -a_0/(h_{20}r^2). \tag{18}$$

The normalization integral is

$$\int_0^{\infty} dr \, r^2[f^2(r) + g^2(r)] = 1. \tag{19}$$

It is easy to see that for the solution with d = –1, the normalization integral diverges at r = 0, so that this solution should be rejected. The solution with d = 0, the normalization integral converges at r = 0, so that this solution should be accepted.

3. NON-ANALYTIC SOLUTION OF THE DIRAC EQUATION INSIDE THE PROTON FOR THE S-STATES OF HYDROGEN ATOMS

Non-analytic solutions of differential equations have been studied for many years – see, e.g., papers [14-20] listed in the reversed chronological order. Here we seek a non-analytic solution of the "interior" Eq. (10) in the form:

$$g_{int}(r) = (1/r^{\gamma})\exp[-(R/r)^{\beta}], \; \beta = \text{const} > 0, \; \gamma = \text{const}, \tag{20}$$

where R is the matching radius, i.e., the radius at which the interior solution should be matched with the singular exterior solution.

It is important to note that this class of solutions embraces the traditional class of analytical solutions as a particular case of $\beta = 0$. Thus, this class of solutions constitutes the generalization of the traditional class of analytical solutions.

Obviously, the function $g_{int}(r)$ from Eq. (20) satisfies Eq. (10) at $r \to 0$. Then according to Eq. (11):

$$f_{int}(r) = [-\gamma/r^{\gamma+1} + \beta R^{\beta}/r^{\gamma+1+\beta}]\exp[-(R/r)^{\beta}]/h_{20}. \quad (21)$$

For the exterior solution, the potential energy of the atomic electron is (in the natural units)

$$V(r) = -\alpha/r, \quad (22)$$

α being the fine structure constant. Since the energy of the states of the principal quantum number n is approximately

$$W \approx 1 - \alpha^2/(2n^2),\ n = 1, 2, 3, \ldots . \quad (23)$$

then $h_1(r)$ and $h_2(r)$ from Eq. (5) can be approximated as follows:

$$h_1(r) \approx \alpha/r - \alpha^2/(2n^2),\ h_2(r) \approx \alpha/r + 2. \quad (24)$$

For the range of r such that

$$R \leq r << 2/\alpha, \quad (25)$$

$h_1(r)$ and $h_2(r)$ can be further simplified to

$$h_1(r) \approx \alpha/r,\ h_2(r) \approx \alpha/r. \quad (26)$$

After taking into account Eqs. (22) and (26), the exterior solution should satisfy the Dirac equation in the following form:

$$r(d^2g/dr^2) + 3(dg/dr) + \alpha^2 g = 0. \quad (27)$$

We seek the solution of the "exterior" Eq. (27) expressed as

$$g_{ext}(r) = Cr^{\delta},\ C = \text{const}. \quad (28)$$

On substituting Eq. (28) in Eq. (27), we get the following equation:

$$\delta^2 + 2\delta + \alpha^2 = 0. \quad (29)$$

Equation (29) has two solutions:

$$\delta_1 = (1 - \alpha^2)^{1/2} - 1 \approx -\alpha^2/2,\ \delta_2 = -(1 - \alpha^2)^{1/2} - 1 \approx -2. \quad (30)$$

For the 1st solution (which we call "regular"):

$$g_{ext}(r) \approx C/r^{\varepsilon},\ f_{ext}(r) \approx -\alpha C/(2r^{\varepsilon}),\ \varepsilon = \alpha^2/2 \approx 2.66\text{x}10^{-5} << 1. \quad (31)$$

For the 2nd solution (which we call "singular"):

$$g_{ext}(r) \approx C/r^2,\ f_{ext}(r) \approx -2C/(\alpha r^2). \quad (32)$$

In Eqs. (31) and (32), for deriving f(r) from g(r), we used Eqs. (7) and (25). The expressions for $g_{ext}(r)$ from Eqs. (31) and (32) reproduce the well-known "small r" results of solving the Dirac equation for the Coulomb potential – see, e.g., the textbook [13].

Now we proceed by matching the singular $g_{ext}(r)$ and $f_{ext}(r)$ from Eq. (32), as well as the logarithmic derivatives of these functions, with the corresponding interior solutions from Eqs. (20) and (21) at r = R. Equating the interior and exterior logarithmic derivatives of the g-component yields

$$-(\gamma - \beta)/R = -2/R, \quad (33)$$

so that

$$\gamma = \beta + 2. \tag{34}$$

Equating the interior and exterior logarithmic derivatives of the f-component and taking into account Eq. (34) yields

$$-(3 - \beta^2/2)/R = -2/R, \tag{35}$$

so that

$$\beta = 2^{1/2}. \tag{36}$$

Thus, the explicit form of the non-analytic interior solution is

$$g_{int}(R,r) = \left(\frac{1}{r^{2+\sqrt{2}}}\right) Exp[-\left(\frac{R}{r}\right)^{\sqrt{2}}] \quad , \tag{36}$$

$$f_{int}(R,r) = \left(\frac{1}{h_{20}}\right)[-\frac{2+\sqrt{2}}{r^{3+\sqrt{2}}} + \frac{\sqrt{2}R^{\sqrt{2}}}{r^{3+2\sqrt{2}}}]Exp[-\left(\frac{R}{r}\right)^{\sqrt{2}}] \quad . \tag{37}$$

By equating $g_{int}(r)$from Eq. (36) to $g_{ext}(r)$ from Eq. (32) at r = R, we find:

$$C = \frac{1}{eR^{\sqrt{2}}}. \tag{38}$$

Thus,

$$g_{ext}(R, r) \approx \frac{1}{eR^{\sqrt{2}}}/r^2,\ f_{ext}(R, r) \approx -2\frac{1}{eR^{\sqrt{2}}}/(\alpha r^2). \tag{39}$$

It turns out that the required match of the above interior and exterior solutions occurs regardless of the particular value of R, as illustrated below.

Figure 1 presents the dependence of the g-component of the wave function on r as we set R = 1 in some arbitrary unit of length. It seen that the interior and exterior parts of the solution are perfectly matched at R = 1.

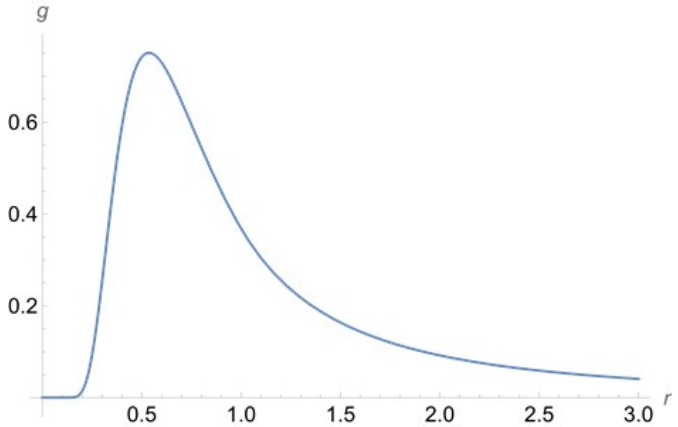

Fig. 1. Dependence of the g-component of the wave function on r as we set R = 1 in some arbitrary unit of length.

For illustrating the perfect match in more detail, we provide Fig. 2 showing, by the solid line, $g_{int}(r)$ from Eq. (36) and, by the dashed line, $g_{ext}(r)$ from Eq. (39). It is seen that at R = 1, there is a smooth transition from the solid line to the dashed line.

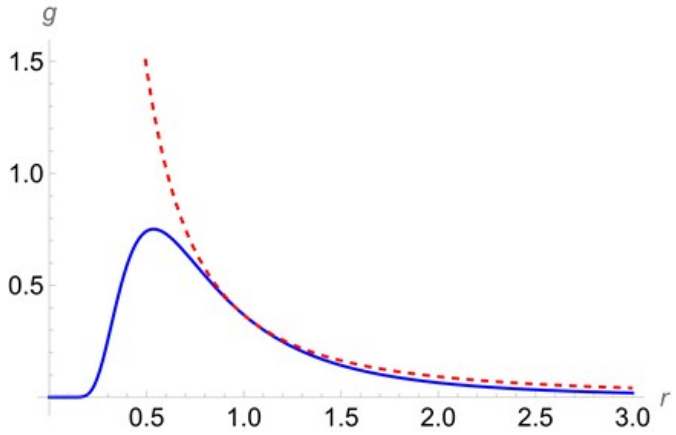

Fig. 2. The plots of $g_{int}(r)$ from Eq. (36) (solid line) and of $g_{ext}(r)$ from Eq. (39) (dashed line) for R = 1.

Figure 3 displays the dependence of the f-component of the wave function on r for R = 1. It seen that the interior and exterior parts of the solution are perfectly matched at R = 1.

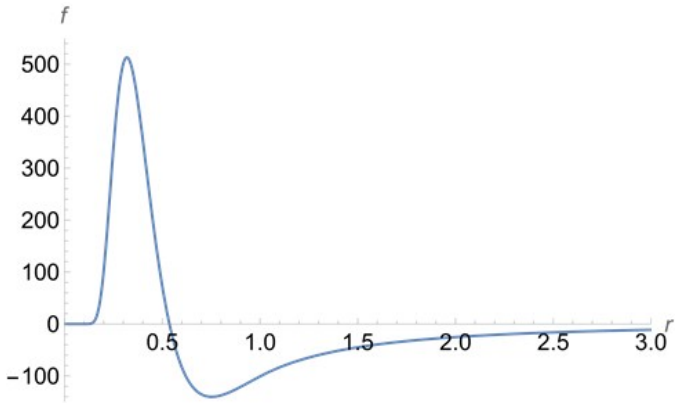

Fig. 3. Dependence of the f-component of the wave function on r for R = 1.

For illustrating the perfect match in more detail, we provide Fig. 4 showing, by the solid line, $f_{int}(r)$ from Eq. (37) and, by the dashed line, $f_{ext}(r)$ from Eq. (39). It is seen that at R = 1, there is a smooth transition from the solid line to the dashed line.

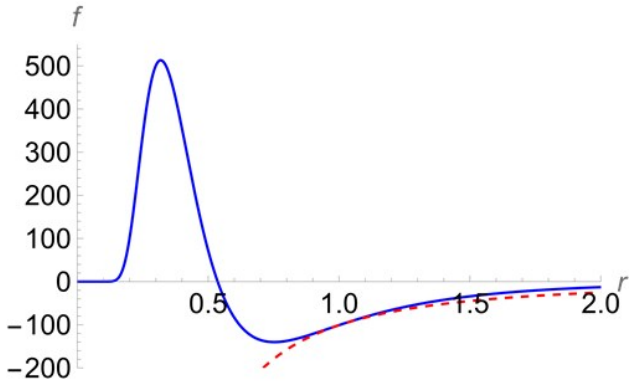

Fig. 4. The plots of $f_{int}(r)$ from Eq. (37) (solid line) and of $f_{ext}(r)$ from Eq. (39) (dashed line) for R = 1.

Now we demonstrate that the required match of the above interior and exterior solutions occurs indeed regardless of the particular value of R. For this purpose, in Fig. 5 we present the dependence of the g-component of the wave function for R = 2 in the same arbitrary unit of length, as for R = 1. It seen that the interior and exterior parts of the solution are perfectly matched at R = 2.

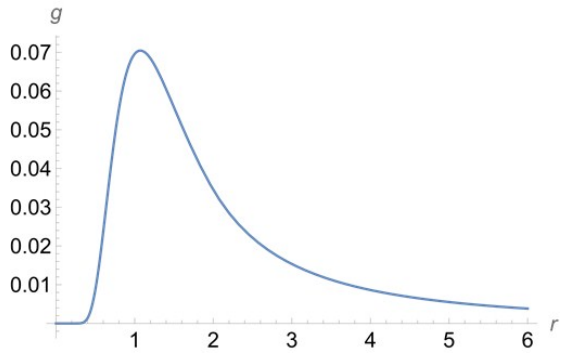

Fig. 5. Dependence of the g-component of the wave function for R = 2 in the same arbitrary unit of length, as for R = 1.

For illustrating the perfect match in more detail, we provide Fig. 6 showing, by the solid line, $g_{int}(r)$ from Eq. (36) and, by the dashed line, $g_{ext}(r)$ from Eq. (39). It is seen that at R = 2, there is a smooth transition from the solid line to the dashed line.

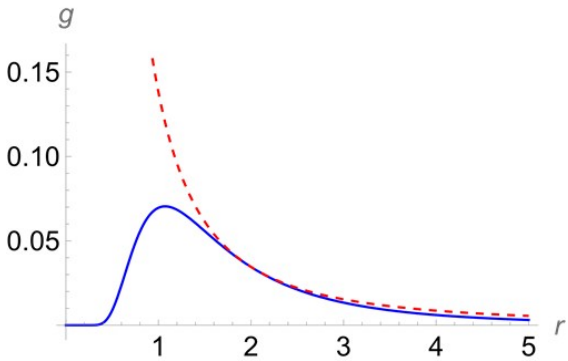

Fig. 6. The plots of $g_{int}(r)$ from Eq. (36) (solid line) and of $g_{ext}(r)$ from Eq. (39) (dashed line) for R = 2.

Figure 7 displays the dependence of the f-component of the wave function on r for R = 2. It seen that the interior and exterior parts of the solution are perfectly matched at R = 2.

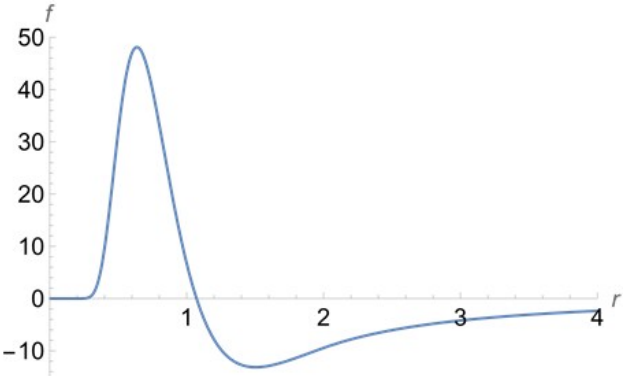

Fig. 7. Dependence of the f-component of the wave function on r for R = 2.

For illustrating the perfect match in more detail, we provide Fig. 8 showing, by the solid line, $f_{int}(r)$ from Eq. (37) and, by the dashed line, $f_{ext}(r)$ from Eq. (39). It is seen that at R = 2, there is a smooth transition from the solid line to the dashed line.

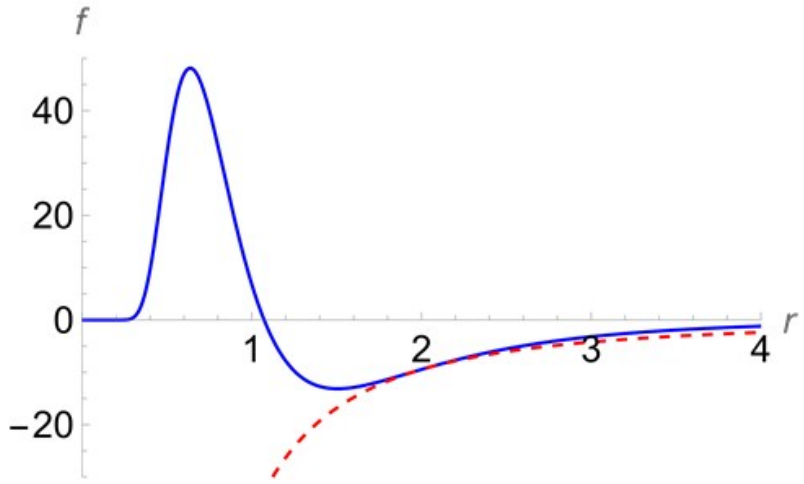

Fig. 8. The plots of $f_{int}(r)$ from Eq. (37) (solid line) and of $g_{ext}(r)$ from Eq. (39) (dashed line) for R = 2.

This completes the detailed theoretical proof of the existence of the SFHA. The rest of the paper concerns applications and has no bearing on the above theoretical proof of the existence of the SFHA.

4. APPLICATION TO RESOLVING THE NEUTRON LIFETIME PUZZLE

The lifetime of free neutrons is perplexing: in the beam experiments ($\tau_{beam} = 888.0 \pm 2.0$ s) it is greater than in the trap experiments ($\tau_{trap} = (877.75 \pm 0.28_{stat} + 0.22/-0.16_{syst})$ s, e.g., according to paper [21], well beyond the error margins. It would have been explained by the *2-body decay* into a hydrogen atom plus antineutrino if the Branching Ratio (BR) for this process – compared to the usual 3-body decay – would be ~ 1%: because in the beam experiments only the protons from the 3-body decay were counted, so that the 2-body decay was missed. However, the previously known theoretical BR (for such 2-body decay) was much smaller: 4×10^{-6} [22].

Alternatively, Fornal and Grinstein [23] hypothesized that neutron might decay into an *unspecified* dark matter (DM) particle. The problem still was that the resulting hypothetical DM particle was not identified. Moreover, Dubbers et al [24] showed that the BR for this process is at least several times smaller than required 1%. In 2024 experiment [25] with the hypothetical dark decay $^6He \longrightarrow {}^4He + n + \chi$, the corresponding BR for free neutrons was shown to be ~ 10^{-5}, while BR ~ 1% is needed for reconciling τ_{trap} and τ_{beam}.

In our papers [26, 27] of 2024, we brought to the attention of the research community that with the allowance for the second solution of Dirac equation for hydrogen atoms, the theoretical BR for the decay into a hydrogen atom (plus antineutrino) is increased by a factor of ~ 3×10^3 to become ~ 1%. This is in the excellent agreement with "experimental" BR = (1.15 ± 0.27)% required for reconciling the above τ_{trap} and τ_{beam}. Thus, it seems that the allowance for the above, enhanced two-body decay of free neutrons solves the neutron lifetime puzzle completely.

In the present paper we provide some details on the above calculations: the details that were not given in our papers [26, 27].*/ First, the wave function, combining the results from Eqs. (36), (37), (39) was complemented by the exponentially declining tail – the tail being similar to the regular solution of the corresponding Dirac equation (see, e.g., the textbook [13]):

$$g_{tail}(r) \sim 2 \exp(-\alpha r), \; f_{tail}(r) \sim \alpha \exp(-\alpha r). \tag{40}$$

Then we calculated the normalization integral N(R):

$$N(R) \approx \int_0^\infty r^2 [g_2^2(R, r) + f_2^2(R, r)] dr. \tag{41}$$

In Eq. (41), $g_2(R, r)$ and $f_2(R, r)$ are the wave functions of the 2nd solution of the Dirac equation (based on Eqs. (36), (37), (39), and (40)), as indicated by the subscript "2".

According to Bahcall [22], the probability P(R) of the 2-body decay of neutrons is proportional to the square absolute value of the wave function of the atomic electron at the proton surface, i.e., at r = R. So, we calculated the following Enhancement Factor (EF)

$$EF(R) = P_2(R)/P_1(R) = [g_{2N}(R, R)^2 + f_{2N}(R, R)^2]/[g_1(R)^2 + f_1(R)^2], \quad (42)$$

where

$$g_{2N}(R, R) = g_2(R, R)/[N(R)]^{1/2}, \; f_{2N}(R, R) = f_2(R, R)/[N(R)]^{1/2}. \quad (43)$$

In Eq. (42), $g_1(R)$ and $f_1(R)$ are the well-known regular solutions of the Dirac equation for hydrogen atoms (see, e.g., the textbook [13]).

On substituting in Eq. (42) as the proton boundary R, the experimental root-mean-square value of the proton radius 0.84 fm = 0.0022 n.u., we obtain EF ~ $3x10^3$ >> 1. This means that the 2-body decay of neutrons should produce overwhelmingly the SFHA, rather than the usual hydrogen atoms. Physically, this is because the wave function of the 2nd solution rises toward the proton surface (from the outside) much more rapidly than the wave function of the 1st solution.

Thus, the branching ratio for the 2-body decay of neutrons, being enhanced by the above value of the EF, becomes ~ 1%, which is indeed in the excellent agreement with the "experimental" branching ratio of (1.15 ± 0.27)% required for reconciling the above τ_{trap} and τ_{beam}. So, in this way, the puzzle of the neutron lifetime seems to be resolved completely.

5. CONCEPTUAL DESIGNS OF THE EXPERIMENTAL VERIFICATION OF THE TWO-BODY DECAY OF NEUTRONS

We can use as the starting point the design proposed by Stephan Paul group from Munich, as presented in the paper by McAndrew et al [28] – see Fig. 9.

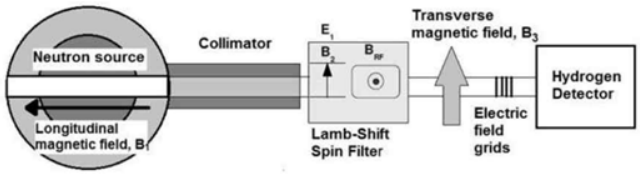

Fig. 9. Design of the experiment proposed in McAndrew et al paper [28].

The neutrons decay inside the through-going beam tube. The hydrogen atoms then pass through the collimator. (The Lamb-shift spin filter is optional.) A transverse magnetic field B_3 then removes a large number of the three-body decay protons and electrons from the beam line.

Here we come to the central point of our suggestion: the resulting hydrogen atoms should be subjected to an electric field (a static field or a laser field) able *to ionize the usual hydrogen atoms from the states 2S, 3S, and so on.* The SFHA cannot and will not be ionized by this field, as explained above.

The theoretically expected result of the 2-body decay of neutrons is 83.2% of hydrogen atoms in the state 1s and 16.8% of hydrogen atoms in the states 2s, 3s, and so on [22]. In the 1st mode of the experiment, the ionizing laser or static electric field should be off. Then all hydrogen atoms should be subjected to an electron beam of the energy ~ (6 – 8) eV to ionize BOTH kinds of hydrogen atoms from the state 2S and higher. (The SFHA can be ionized by the electron beam, just as the usual hydrogen atoms.) Then the resulting protons should be deflected (by a static electric field) and counted.

In the 2nd mode of the experiment, the ionizing laser or static electric field should be on. Then again all hydrogen atoms should be subjected to an electron beam of the energy ~ (6 – 8) eV to ionize *both* kinds of hydrogen atoms from the state 2S and higher. Then the resulting protons should be deflected and counted. If the 2nd count of protons would be approximately the same as the 1st count, this would confirm that *the 2-body decay of neutrons produces*

overwhelmingly the SFHA (rather than the usual hydrogen atoms). If the 2nd count of protons would be zero or much less than the 1st count, this would mean: no SFHA.

Alternatively, the experiment could be performed without using the electron beam at the last stage of the experiment, as follows. In the 1st mode of the experiment, all the resulting hydrogen atoms should be counted (e.g., by using a microcalorimeter as the detector). In the 2nd mode of the experiment, before detecting hydrogen atoms, they should be subjected to *a static or laser field able to ionize the usual hydrogen atoms from the states 2s, 3s, and so on*, and then to count the remaining hydrogen atoms. (The SFHA will not get ionized.) If the 2nd count would be approximately the same as the 1st count (within the accuracy of few percent), this would confirm that *the 2-body decay of neutrons produces overwhelmingly the SFHA*. If the 2nd count would be by about 17% smaller than the 1st count, this would mean: no SFHA. As for the detector of hydrogen atoms, it could be, e.g., a microcalorimeter, as proposed by Shuo et al [29].

Here are some details on ionizing the usual hydrogen atoms by a laser or static electric field. For ionizing the usual hydrogen atoms from the states 2s, 3s, and so on, it should be enough to use a laser of the intensity ~ 5×10^{11} W/cm^2 . For enabling the increase of the laser focus spot to the size of the hydrogen beam cross-section, it should be enough to use a laser of the intensity ~ 5×10^{13} W/cm^2. By now laser intensities ~ 10^{21} W/cm^2 are achieved; so, the Nd:YAG laser providing ~ 10^{14} W/cm^2 is readily available from commercial sources.

Alternatively, instead of the laser field, a static electric field ~ 20 MV/cm can be used for this purpose.

Another starting point could be the layout of the beam-type experiment by Nico et al [30] – see Fig. 10.

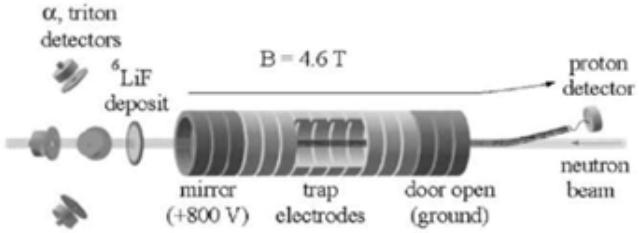

Fig. 10. The layout of the beam-type experiment by Nico et al [30].

In this experiment, the trapping region intercepts the entire neutron beam and neutrons decay inside this volume in the 3-body and 2-body ways. In the trapping mode, the protons resulting from the 3-body decay are confined there. Then (as in the counting mode) door electrodes are grounded, and a graduated potential is imposed on the central electrodes to flush out protons.

Here we come to the central point of our suggestion: the hydrogen atoms, resulting from the 2-body decay, *should be subjected to an electron beam of the energy 11 – 13 eV* to excite both kinds of hydrogen atoms *into the states of the principal quantum number n = 2 and higher*. In the 1st mode of the experiment, the hydrogen atoms should be subjected to another electron beam of the energy ~ (6 – 8) eV to ionize *both* kinds of hydrogen atoms from the state 2S and higher, followed by counting the resulting protons.

In the 2nd mode of the experiment, first the usual hydrogen atoms in the state 2S and higher should be quenched out by an electric field that would mix the S- and P-states, followed by the radiative decay into the ground state. (The SFHA cannot be quenched: the SFHA does not have the P-states.) Then the SFHA in the state 2S and higher, should be subjected to the second electron beam of the energy ~ (6 – 8) eV to ionize them, followed by counting the resulting protons.

If the 2nd count of protons would be approximately the same as the 1st count, this would confirm that *the 2-body decay of neutrons produces overwhelmingly the SFHA* (rather than the usual hydrogen atoms). If the 2nd count of protons would be zero or much less than the 1st count, this would mean: no SFHA.

6. CONCLUSIONS

We obtained the explicit form of the solution of the Dirac equation inside the proton for the S-states – the solution that at the proton boundary matches the corresponding singular solution, as required by quantum mechanics: both the

wave function and its derivative are continuous at the boundary. We demonstrated that such solution inside the proton can be (and is) obtained within the class of functions that are *non-analytic* at r = 0 – in distinction to the conventional practice of limiting the search for the solution by the class of analytic functions, i.e., by functions that can be adequately represented by their expansion into the Laurent series.

We applied the obtained results to the resolution of the neutron lifetime puzzle. We demonstrated that the 2-body decay of neutrons produces overwhelmingly the SFHA (rather than the usual hydrogen atoms). By showing that the enhanced in this way branching ratio for the 2-body decay of neutrons (compared to the 3-body decay) is in the excellent agreement with the branching ratio required for reconciling the neutron lifetime values measured in the trap and beam experiments, we resolved the neutron lifetime puzzle completely.

Finally, we provided the conceptual designs of the experiment that would constitute both the first detection of the 2-body decay of neutrons and the verification that that the 2-body decay of neutrons produces overwhelmingly the SFHA. Thus, our results seem to be important both from the theoretical and experimental viewpoints. For example, they have profound cosmological consequences. They lead to viewing neutron stars in a new light: as the generators of the baryonic DM in the Universe, as presented in paper [27].

Appendix A. The experimental charge density distribution inside the proton

The most recent Charge Density Distribution (CDD) inside protons ρ(r), deduced from the corresponding experimental electric form-factors $G_e(q)$, was presented in 2018 by Sick [31] – see Fig. A.1.

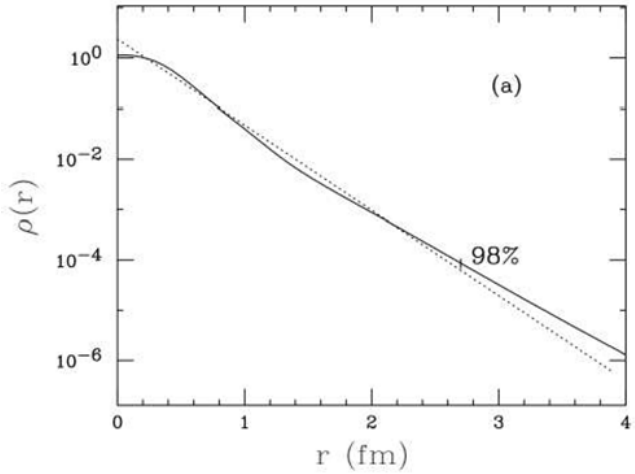

Fig. A.1. The experimental charge density distribution inside the protons according to Sick [31]: the distribution corresponding to the dipole form factor (dotted line) and a more realistic one (solid line) resulting from the fit to the *experimental* electron scattering data. The mark 98% shows that integrating from 0 to 2.7 fm yields 98% of the rms-radius of protons.

The experimental $G_e(q)$ were taken from a variety of world data. In the non-relativistic limit, ρ(r) is related to $G_e(q)$ by the Fourier-transform:

$$\rho(r) = [1/(2\pi^2 r)] \int_0^\infty G_e(q) \sin(qr)\, q\, dq \qquad (A.1)$$

The proton form factor is roughly described by the dipole shape:

$$G_D(q) = 1/(1 + q^2 R_D^2/12)^2 , \qquad (A.2)$$

where R_D is the corresponding rms proton charge radius. The CDD corresponding to this form factor has the shape of an exponential:

$$\rho_D(r) \propto \exp(-12^{1/2} r/R_D). \qquad (A.3)$$

It is seen that *the experimental CDD in protons* (solid line) *has the maximum at r = 0* and then monotonically falls-off to the periphery. This kind of the CDD yields the potential satisfying, as a particular case, the general condition

from Eq. (2), under which the wave functions inside the proton can be matched at the proton boundary with the wave function of the singular solution outside the proton.

The commonly used characteristic parameter of any distribution (or of a spectral line shape) is its Half Width at Half Maximum (HWHM). For the experimental CDD shown by the solid line in Fig. A.1, we found HWHM ≈ 0.32 fm ≈ 0.00089 n.u.

Notes

*/ There was a misprint in the expression for $g_{int}(r)$ in Eq. (2) from paper [26] and in the corresponding Eq.(3) from paper [27]: in the denominator, instead of r should have been r^2. This misprint was "inherited" from paper [1] where in the expression for $g_{int}(r)$ in Eq. (17), the power of r in the denominator should have been increased by 1. In the above papers, the subsequent calculations were performed by the correct formulas, so that these misprints did not affect the results

References

1. E. Oks, J. Phys. B: At. Mol. Opt. Phys. **2001**, *34,* 2235
2. M. Gryzinski, *Phys. Rev.* **1965**, *138*, A336
3. V. Fock, *Z. Physik* **1935**, *98*, 145
4. G.G. Simon et al, *Nucl. Phys.* A **1980**, *333***,** 381
5. D.H. Perkins, *Introduction to High Energy Physics* (Menlo Park, CA: Addison-Wesley) **1987**, section 6.5
6. R.P. Feynman, 1989 *Photon-Hadron Interactions* (Redwood City, CA: Addison-Wesley) **1989**, Lecture 24
7. E. Oks, *Research in Astronomy and Astrophysics* **2020**, *20(7)*, 109
8. E. Oks, *Atoms* **2020**, *8*, 33
9. J.D. Bowman et al, *Nature* **2018**, *555*, 67
10. R. Barkana, *Nature* **2018**, *555*, 71
11. S.S. McGaugh *Research Notes of the Amer. Astron. Soc.* **2018**, 2, 37
12. E. Oks, Int. J. Mod. Phys. D **2025** (accepted).
13. M.E. Rose, *Relativistic Electron Theory* (New York: Wiley) **1961**, sections 28, 29, 39
14. F. Mohammadi, J. Math. Extension **2014**, *8*, 55
15. S.Gh. Hosseini and F. Mohammadi, Appl. Math. Sciences **2011**, *5*, 2537
16. F. Mohammadi et al, Intern. J. of Systems Science **2011**, *42*, 579
17. P. Byers and A. Himonas, Abstract and Applied Analysis **2004**, *6*, 453
18. M. D. Bronshtein, Uspekhi Mat. Nauk **1975**, *30*, Issue 1, 227
19. O. A. Oleinik and E. V. Radkevich, Uspekhi Mat. Nauk **1973**, *28*, Issue 3, 191
20. O. A. Oleinik and E. V. Radkevich, Uspekhi Mat. Nauk **1972**, *27*, 247
21. F.M. Gonzalez et al, Phys. Rev. Lett. **2021**, *127*, 162501
22. J.N. Bahcall, Phys. Rev. **1961**, *124*, 495
23. B. Fornal and B. Grinstein, Phys. Rev. Lett. **2018**, *120*, 191801
24. D. Dubbers et al, Phys. Lett. B **2019**, 791, 6
25. M. Le Joubioux et al, Phys. Rev. Lett. **2024**, *132*, 132501
26. E. Oks, 2024 Intern. Review Atom. Molec. Phys. **2024**, *15*, 49
27. E. Oks, New Astronomy **2024**, *113*, 102275
28. J. McAndrew et al, Phys. Procedia **2014**, *51*, 37
29. Zh. Shuo et al, **2022** https://arxiv.org/abs/2210.02314
30. J.S. Nico et al, Phys. Rev. C **2005**, *71*, 055502
31. I. Sick, Atoms **2018**, *6*, 2